# 6 Electron–positron annihilation

Experimental results from electron–positron colliders have been central to the development and understanding of the Standard Model. In this chapter, the derivation of the cross section for $e^+e^- \to \mu^+\mu^-$ annihilation is used as an example of a calculation in QED. The cross section is first calculated using helicity amplitudes to evaluate the matrix elements, highlighting the underlying spin structure of the interaction. In the final starred section, the more abstract trace formalism is introduced.

## 6.1 Calculations in perturbation theory

In QED, the dominant contribution to a cross section or decay rate is usually the Feynman diagram with the fewest number of interaction vertices, known as the lowest-order (LO) diagram. For the annihilation process $e^+e^- \to \mu^+\mu^-$, there is just a single lowest-order QED diagram, shown in Figure 6.1. In this diagram there are two QED interaction vertices, each of which contributes a factor $ie\gamma^\mu$ to the matrix element. Therefore, regardless of any other considerations, the matrix element squared $|\mathcal{M}|^2$ will be proportional to $e^4$ or equivalently $|\mathcal{M}|^2 \propto \alpha^2$, where $\alpha$ is the dimensionless fine-structure constant $\alpha = e^2/4\pi$. In general, each QED vertex contributes a factor of $\alpha$ to the expressions for cross sections and decay rates.

In addition to the lowest-order diagram of Figure 6.1, there are an infinite number of higher-order-diagrams resulting in the same final state. For example, three of the next-to-leading-order (NLO) diagrams for $e^+e^- \to \mu^+\mu^-$, each with four interaction vertices, are shown in Figure 6.2. Taken in isolation, the matrix element squared for each of these diagrams has a factor $\alpha$ for each of the four QED vertices, and hence $|\mathcal{M}|^2 \propto \alpha^4$. However, in quantum mechanics the individual Feynman diagrams for a particular process can not be taken in isolation; the total amplitude $\mathcal{M}_{fi}$ for a particular process is the sum of all individual amplitudes giving the *same final state*. In the case of $e^+e^- \to \mu^+\mu^-$, this sum can be written as

$$\mathcal{M}_{fi} = \mathcal{M}_{\text{LO}} + \sum_j \mathcal{M}_{1,j} + \cdots , \tag{6.1}$$

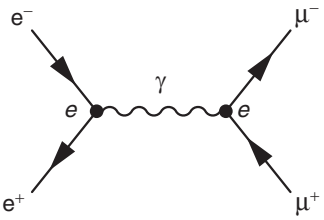


Fig. 6.1 The lowest-order Feynman diagram for the QED annihilation process $e^+e^- \to \mu^+\mu^-$.

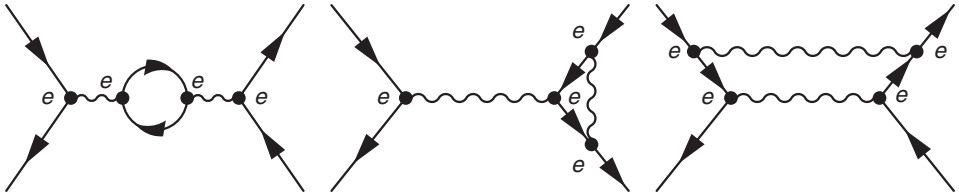


Fig. 6.2 Three of the $O(\alpha^4)$ Feynman diagrams contributing the QED annihilation process $e^+e^- \to \mu^+\mu^-$.

where $\mathcal{M}_{\rm LO}$ is the matrix element for the single lowest-order (LO) diagram of Figure 6.1, $\mathcal{M}_{1,j}$ are the matrix elements for the NLO diagrams with four interaction vertices, including those of Figure 6.2, and the dots indicate the higher-order diagrams with more than four vertices. The dependence of the each of the terms in (6.1) on $\alpha$ can be shown explicitly by writing it as

$$\mathcal{M}_{fi} = \alpha M_{\rm LO} + \alpha^2 \sum_j M_{1,j} + \cdots ,$$

where the various powers of the coupling constant $\alpha$ have been factored out of the matrix element, such that $\mathcal{M}_{\rm LO}$ is written as $\alpha M_{\rm LO}$, etc.

Physical observables, such as decay rates and cross sections, depend on the matrix element squared given by

$$\begin{aligned} |\mathcal{M}_{fi}|^2 &= \left(\alpha M_{\rm LO} + \alpha^2 \sum_j M_{1,\rm j} + \cdots\right)\left(\alpha M^*_{\rm LO} + \alpha^2 \sum_k M^*_{1,\rm k} + \cdots\right) \\ &= \alpha^2 |M_{\rm LO}|^2 + \alpha^3 \sum_j \left(M_{\rm LO} M^*_{1,j} + M^*_{\rm LO} M_{1,j}\right) + \alpha^4 \sum_{jk} M_{1,j} M^*_{1,\rm k} + \cdots . \end{aligned} \tag{6.2}$$

In general, the individual amplitudes are complex and the contributions from different diagrams can interfere either positively or negatively. Equation (6.2) gives the QED perturbation expansion in terms of powers of $\alpha$. For QED, the dimensionless coupling constant $\alpha \approx 1/137$ is sufficiently small that this series converges rapidly and is dominated by the LO term. The interference between the lowest-order diagram and the NLO diagrams, terms such as $(M_{\rm LO} M^*_{1,j} + M^*_{\rm LO} M_{1,j})$, are suppressed by a factor of $\alpha \approx 1/137$ relative to the lowest-order term. Hence, if all higher-order

terms are neglected, it is reasonable to expect QED calculations to be accurate to $O(1\%)$. For this reason, only the lowest-order diagram(s) will be considered for the calculations in this book, although the impact of the higher-order diagrams will be discussed further in Chapter 10 in the context of renormalisation.

## 6.2 Electron–positron annihilation

The matrix element for the lowest-order diagram for the process $e^+e^- \to \mu^+\mu^-$ is given in (5.20),

$$\mathcal{M} = -\frac{e^2}{q^2} g_{\mu\nu} [\bar{v}(p_2)\gamma^\mu u(p_1)][\bar{u}(p_3)\gamma^\nu v(p_4)] \tag{6.3}$$

$$= -\frac{e^2}{q^2} g_{\mu\nu} j_e^\mu j_\mu^\nu, \tag{6.4}$$

where the electron and muon four-vector currents are defined as

$$j_e^\mu = \bar{v}(p_2)\gamma^\mu u(p_1) \quad \text{and} \quad j_\mu^\nu = \bar{u}(p_3)\gamma^\nu v(p_4). \tag{6.5}$$

The four-momentum of the virtual photon is determined by conservation of energy and momentum at the interaction vertex, $q = p_1 + p_2 = p_3 + p_4$, and therefore $q^2 = (p_1 + p_2)^2 = s$, where $s$ is the centre-of-mass energy squared. Hence the matrix element of (6.4) can be written as

$$\mathcal{M} = -\frac{e^2}{s} j_e \cdot j_\mu. \tag{6.6}$$

Assuming that the electron and positron beams have equal energies, which has been the case for the majority of high-energy $e^+e^-$ colliders, the centre-of-mass energy is simply twice the beam energy, $\sqrt{s} = 2E_{\text{beam}}$.

### 6.2.1 Spin sums

To calculate the $e^+e^- \to \mu^+\mu^-$ cross section, the matrix element of (6.6) needs to be evaluated taking into account the possible spin states of the particles involved. Because each of the $e^+$, $e^-$, $\mu^+$ and $\mu^-$ can be in one of two possible helicity states, there are four possible helicity configurations in the initial state, shown Figure 6.3, and four possible helicity configurations in the $\mu^+\mu^-$ final state. Hence, the process $e^+e^- \to \mu^+\mu^-$ consists of sixteen possible *orthogonal* helicity combinations, each of

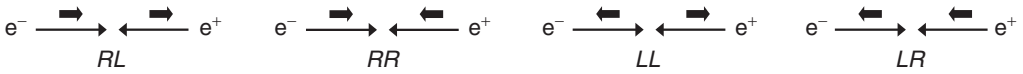


Fig. 6.3 The four possible helicity combinations in the $e^+e^-$ initial state.

which constitutes a separate physical process, for example $e^+_\uparrow e^-_\uparrow \to \mu^+_\uparrow \mu^-_\uparrow$ (denoted $RR \to RR$) and $e^+_\uparrow e^-_\uparrow \to \mu^+_\uparrow \mu^-_\downarrow$. Because the helicity states involved are orthogonal, the processes for the different helicity configurations do not interfere and the matrix element squared for each of the sixteen possible helicity configurations can be considered independently.

For a particular initial-state spin configuration, the total $e^+e^- \to \mu^+\mu^-$ annihilation rate is given by the sum of the *rates* for the four possible $\mu^+\mu^-$ helicity states (each of which is a separate process). Therefore, for a given *initial-state* helicity configuration, the cross section is obtained by taking the sum of the four corresponding $|\mathcal{M}|^2$ terms. For example, for the case where the colliding electron and positron are both in right-handed helicity states,

$$\sum |\mathcal{M}_{RR}|^2 = |\mathcal{M}_{RR\to RR}|^2 + |\mathcal{M}_{RR\to RL}|^2 + |\mathcal{M}_{RR\to LR}|^2 + |\mathcal{M}_{RR\to LL}|^2.$$

In most $e^+e^-$ colliders, the colliding electron and positron beams are unpolarised, which means that there are equal numbers of positive and negative helicity electrons/positrons present in the initial state. In this case, the helicity configuration for a particular collision is equally likely to occur in any one of the four possible helicity states of the $e^+e^-$ initial state. This is accounted for by defining the spin-averaged summed matrix element squared,

$$\begin{aligned}\langle|\mathcal{M}_{fi}|^2\rangle &= \frac{1}{4}\left(|\mathcal{M}_{RR}|^2 + |\mathcal{M}_{RL}|^2 + |\mathcal{M}_{LR}|^2 + |\mathcal{M}_{LL}|^2\right)\\ &= \frac{1}{4}\left(|\mathcal{M}_{RR\to RR}|^2 + |\mathcal{M}_{RR\to RL}|^2 + \cdots + |\mathcal{M}_{RL\to RR}|^2 + \cdots\right),\end{aligned}$$

where the factor $\frac{1}{4}$ accounts for the average over the four possible initial-state helicity configurations. In general, the spin-averaged matrix element is given by

$$\langle|\mathcal{M}_{fi}|^2\rangle = \frac{1}{4}\sum_{\text{spins}} |\mathcal{M}|^2,$$

where the sum corresponds to all possible helicity configurations. Consequently, to evaluate the $e^+e^- \to \mu^+\mu^-$ cross section, it is necessary to calculate the matrix element of (6.6) for sixteen helicity combinations. This sum can be performed in two ways. One possibility is to use the trace techniques described in Section 6.5, where the sum is calculated directly using the properties of the Dirac spinors. The second possibility is to calculate each of the sixteen individual helicity amplitudes. This direct calculation of the helicity amplitudes involves more steps, but has the

advantages of being conceptually simpler and of leading to a deeper physical understanding of the helicity structure of the QED interaction.

### 6.2.2 Helicity amplitudes

In the limit where the masses of the particles can be neglected, $\sqrt{s} \gg m_\mu$, the four-momenta in the process $e^+e^- \to \mu^+\mu^-$, as shown Figure 6.4, can be written

$$p_1 = (E, 0, 0, E), \tag{6.7}$$
$$p_2 = (E, 0, 0, -E), \tag{6.8}$$
$$p_3 = (E, E\sin\theta, 0, E\cos\theta), \tag{6.9}$$
$$p_4 = (E, -E\sin\theta, 0, -E\cos\theta), \tag{6.10}$$

where, with no loss of generality, the final state $\mu^-$ and $\mu^+$ are taken to be produced with azimuthal angles of $\phi = 0$ and $\phi = \pi$ respectively.

The spinors appearing in the four-vector currents of (6.5) are the ultra-relativistic ($E \gg m$) limit of the helicity eigenstates of (4.67):

$$u_\uparrow = \sqrt{E}\begin{pmatrix} c \\ se^{i\phi} \\ c \\ se^{i\phi} \end{pmatrix},\ u_\downarrow = \sqrt{E}\begin{pmatrix} -s \\ ce^{i\phi} \\ s \\ -ce^{i\phi} \end{pmatrix},\ v_\uparrow = \sqrt{E}\begin{pmatrix} s \\ -ce^{i\phi} \\ -s \\ ce^{i\phi} \end{pmatrix},\ v_\downarrow = \sqrt{E}\begin{pmatrix} c \\ se^{i\phi} \\ c \\ se^{i\phi} \end{pmatrix}, \tag{6.11}$$

where $s = \sin\frac{\theta}{2}$ and $c = \cos\frac{\theta}{2}$. The two possible spinors for initial-state electron with $(\theta = 0, \phi = 0)$ and for the initial-state positron with $(\theta = \pi, \phi = \pi)$ are

$$u_\uparrow(p_1) = \sqrt{E}\begin{pmatrix} 1 \\ 0 \\ 1 \\ 0 \end{pmatrix},\ u_\downarrow(p_1) = \sqrt{E}\begin{pmatrix} 0 \\ 1 \\ 0 \\ -1 \end{pmatrix},\ v_\uparrow(p_2) = \sqrt{E}\begin{pmatrix} 1 \\ 0 \\ -1 \\ 0 \end{pmatrix},\ v_\downarrow(p_2) = \sqrt{E}\begin{pmatrix} 0 \\ -1 \\ 0 \\ -1 \end{pmatrix}.$$

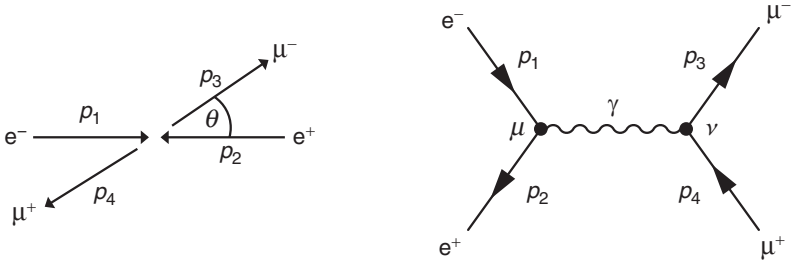


Fig. 6.4 The QED annihilation process $e^+e^- \to \mu^+\mu^-$ viewed in the centre-of-mass frame and the corresponding lowest-order Feynman diagram.

The spinors for the final-state particles are obtained by using the spherical polar angles $(\theta, 0)$ for the $\mu^-$ and $(\pi-\theta, \pi)$ for the $\mu^+$. Using the trigonometric relations

$$\sin\left(\frac{\pi-\theta}{2}\right) = \cos\left(\frac{\theta}{2}\right), \quad \cos\left(\frac{\pi-\theta}{2}\right) = \sin\left(\frac{\theta}{2}\right) \quad \text{and} \quad e^{i\pi} = -1,$$

the spinors for the two possible helicity states of the final-state $\mu^+$ and $\mu^-$ are

$$u_\uparrow(p_3) = \sqrt{E}\begin{pmatrix} c \\ s \\ c \\ s \end{pmatrix}, \; u_\downarrow(p_3) = \sqrt{E}\begin{pmatrix} -s \\ c \\ s \\ -c \end{pmatrix}, \; v_\uparrow(p_4) = \sqrt{E}\begin{pmatrix} c \\ s \\ -c \\ -s \end{pmatrix}, \; v_\downarrow(p_4) = \sqrt{E}\begin{pmatrix} s \\ -c \\ s \\ -c \end{pmatrix}.$$

### 6.2.3 The muon and electron currents

The matrix element for a particular helicity combination is obtained from (6.6),

$$\mathcal{M} = -\frac{e^2}{s} j_e \cdot j_\mu,$$

where the corresponding four-vector currents of (6.5) are defined in terms of the above spinors for the helicity eigenstates. The muon current, $j_\mu^\nu = \overline{u}(p_3)\gamma^\nu v(p_4)$, needs to be evaluated for the four possible final-state helicity combinations shown in Figure 6.5. Using the Dirac–Pauli representation of the $\gamma$-matrices (4.35), it is straightforward to show that, for any two spinors $\psi$ and $\phi$, the components of $\overline{\psi}\gamma^\mu\phi \equiv \psi^\dagger\gamma^0\gamma^\mu\phi$ are

$$\overline{\psi}\gamma^0\phi = \psi^\dagger\gamma^0\gamma^0\phi = \psi_1^*\phi_1 + \psi_2^*\phi_2 + \psi_3^*\phi_3 + \psi_4^*\phi_4, \tag{6.12}$$

$$\overline{\psi}\gamma^1\phi = \psi^\dagger\gamma^0\gamma^1\phi = \psi_1^*\phi_4 + \psi_2^*\phi_3 + \psi_3^*\phi_2 + \psi_4^*\phi_1, \tag{6.13}$$

$$\overline{\psi}\gamma^2\phi = \psi^\dagger\gamma^0\gamma^2\phi = -i(\psi_1^*\phi_4 - \psi_2^*\phi_3 + \psi_3^*\phi_2 - \psi_4^*\phi_1), \tag{6.14}$$

$$\overline{\psi}\gamma^3\phi = \psi^\dagger\gamma^0\gamma^3\phi = \psi_1^*\phi_3 - \psi_2^*\phi_4 + \psi_3^*\phi_1 - \psi_4^*\phi_2. \tag{6.15}$$

Using these relations, the four components of the four-vector current $j_\mu$ can be determined by using the spinors for a particular helicity combination. For example, for the *RL* combination where the $\mu^-$ is produced in a right-handed helicity state and the $\mu^+$ is produced in a left-handed helicity state, the appropriate spinors are $u_\uparrow(p_3)$ and $v_\downarrow(p_4)$. In this case, from Equations (6.12)–(6.15), the components of

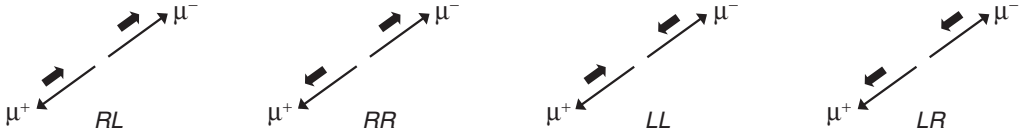


Fig. 6.5 The four possible helicity combinations for the $\mu^+\mu^-$ final state.

the muon current are

$$
\begin{aligned}
j_\mu^0 &= \bar{u}_\uparrow(p_3)\gamma^0 v_\downarrow(p_4) = E(cs - sc + cs - sc) = 0,\\
j_\mu^1 &= \bar{u}_\uparrow(p_3)\gamma^1 v_\downarrow(p_4) = E(-c^2 + s^2 - c^2 + s^2) = 2E(s^2 - c^2) = -2E\cos\theta,\\
j_\mu^2 &= \bar{u}_\uparrow(p_3)\gamma^2 v_\downarrow(p_4) = -iE(-c^2 - s^2 - c^2 - s^2) = 2iE,\\
j_\mu^3 &= \bar{u}_\uparrow(p_3)\gamma^3 v_\downarrow(p_4) = E(cs + sc + cs + sc) = 4Esc = 2E\sin\theta.
\end{aligned}
$$

Hence, the four-vector current for the helicity combination $\mu^-_\uparrow\mu^+_\downarrow$ is

$$
j_{\mu,RL} = \bar{u}_\uparrow(p_3)\gamma^\nu v_\downarrow(p_4) = 2E(0, -\cos\theta, i, \sin\theta).
$$

Repeating the calculation for the other three $\mu^+\mu^-$ helicity combinations gives

$$
\begin{aligned}
j_{\mu,RL} &= \bar{u}_\uparrow(p_3)\gamma^\nu v_\downarrow(p_4) = 2E(0, -\cos\theta, i, \sin\theta), &(6.16)\\
j_{\mu,RR} &= \bar{u}_\uparrow(p_3)\gamma^\nu v_\uparrow(p_4) = (0,0,0,0),\\
j_{\mu,LL} &= \bar{u}_\downarrow(p_3)\gamma^\nu v_\downarrow(p_4) = (0,0,0,0),\\
j_{\mu,LR} &= \bar{u}_\downarrow(p_3)\gamma^\nu v_\uparrow(p_4) = 2E(0, -\cos\theta, -i, \sin\theta). &(6.17)
\end{aligned}
$$

Hence, in the limit where $E \gg m_\mu$, only two of the four $\mu^+\mu^-$ helicity combinations lead to a non-zero four-vector current. This important feature of QED is related to the chiral nature of the interaction, as discussed in Section 6.4.

The electron currents for the four possible initial-state helicity configurations can be evaluated directly using (6.12)–(6.15). Alternatively, the electron currents can be obtained by noting that they differ from the form of the muon currents only in the order in which the particle and antiparticle spinors appear, $j_e^\mu = \bar{v}(p_2)\gamma^\mu u(p_1)$ compared to $j_\mu^\nu = \bar{u}(p_3)\gamma^\nu v(p_4)$. The relationship between $\bar{v}\gamma^\mu u$ and $\bar{u}\gamma^\mu v$ can be found by taking the Hermitian conjugate of the muon current to give

$$
\begin{aligned}
[\bar{u}(p_3)\gamma^\mu v(p_4)]^\dagger &= \left[u(p_3)^\dagger\gamma^0\gamma^\mu v(p_4)\right]^\dagger\\
&= v(p_4)^\dagger\gamma^{\mu\dagger}\gamma^{0\dagger}u(p_3) && \text{using } (AB)^\dagger = B^\dagger A^\dagger\\
&= v(p_4)^\dagger\gamma^{\mu\dagger}\gamma^0 u(p_3) && \text{since } \gamma^{0\dagger} = \gamma^0\\
&= v(p_4)^\dagger\gamma^0\gamma^\mu u(p_3) && \text{since } \gamma^{\mu\dagger}\gamma^0 = \gamma^0\gamma^\mu\\
&= \bar{v}(p_4)\gamma^\mu u(p_3).
\end{aligned}
$$

The effect of taking the Hermitian conjugate of the QED current is to swap the order in which the spinors appear in the current. Because each element of the four-vector current, labelled by the index $\mu$, is just a complex number, the elements of the four-vector current for $\bar{v}\gamma^\mu u$ are given by the complex conjugates of the corresponding elements of $\bar{u}\gamma^\mu v$. Therefore from (6.16) and (6.17),

$$
\begin{aligned}
\bar{v}_\downarrow(p_4)\gamma^\mu u_\uparrow(p_3) &= [\bar{u}_\uparrow(p_3)\gamma^\mu v_\downarrow(p_4)]^* = 2E(0, -\cos\theta, -i, \sin\theta)\\
\bar{v}_\uparrow(p_4)\gamma^\mu u_\downarrow(p_3) &= [\bar{u}_\downarrow(p_3)\gamma^\mu v_\uparrow(p_4)]^* = 2E(0, -\cos\theta, i, \sin\theta).
\end{aligned}
$$

By setting $\theta = 0$, it follows that the two non-zero electron currents are

$$j_{e,RL} = \bar{v}_{\downarrow}(p_2)\gamma^{\mu}u_{\uparrow}(p_1) = 2E(0,-1,-i,0), \tag{6.18}$$
$$j_{e,LR} = \bar{v}_{\uparrow}(p_2)\gamma^{\mu}u_{\downarrow}(p_1) = 2E(0,-1,i,0). \tag{6.19}$$

Furthermore, from $j_{\mu,LL} = j_{\mu,RR} = 0$, it follows that $j_{e,LL}$ and $j_{e,RR}$ are also zero.

### 6.2.4 The $e^+e^- \to \mu^+\mu^-$ cross section

In the limit $E \gg m$, only two of the four helicity combinations for both the initial and final state lead to non-zero four-vector currents. Therefore, in the process $e^+e^- \to \mu^+\mu^-$ only the four helicity combinations shown in Figure 6.6 give non-zero matrix elements. For each of these four helicity combinations, the matrix element is obtained from

$$\mathcal{M} = -\frac{e^2}{s} j_e \cdot j_\mu .$$

For example, the matrix element $\mathcal{M}_{RL\to RL}$ for the process $e^-_{\uparrow}e^+_{\downarrow} \to \mu^-_{\uparrow}\mu^+_{\downarrow}$ is determined by the scalar product of the currents

$$j^{\mu}_{e,RL} = \bar{v}_{\downarrow}(p_2)\gamma^{\mu}u_{\uparrow}(p_1) = 2E(0,-1,-i,0),$$
and $$j^{\nu}_{\mu,RL} = \bar{u}_{\uparrow}(p_3)\gamma^{\nu}v_{\downarrow}(p_4) = 2E(0,-\cos\theta,i,\sin\theta).$$

Taking the four-vector scalar product $j_{e,RL}\cdot j_{\mu,RL}$ and writing $s = 4E^2$ gives

$$\begin{aligned}\mathcal{M}_{RL\to RL} &= -\frac{e^2}{s}[2E(0,-1,-i,0)]\cdot[2E(0,-\cos\theta,i,\sin\theta)]\\ &= e^2(1+\cos\theta)\\ &= 4\pi\alpha(1+\cos\theta).\end{aligned}$$

Using the muon and electron currents of (6.16)–(6.19), it follows that the matrix elements corresponding to the four helicity combinations of Figure 6.6 are

$$|\mathcal{M}_{RL\to RL}|^2 = |\mathcal{M}_{LR\to LR}|^2 = (4\pi\alpha)^2(1+\cos\theta)^2, \tag{6.20}$$
$$|\mathcal{M}_{RL\to LR}|^2 = |\mathcal{M}_{LR\to RL}|^2 = (4\pi\alpha)^2(1-\cos\theta)^2, \tag{6.21}$$

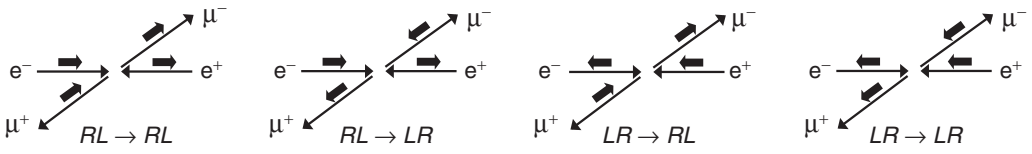


Fig. 6.6 The four helicity combinations for $e^+e^- \to \mu^+\mu^-$ that in the limit $E \gg m$ give non-zero matrix elements.

where $\theta$ is the angle of the outgoing $\mu^-$ with respect to the incoming $e^-$ direction. The spin-averaged matrix element for the process $e^+e^- \to \mu^+\mu^-$ is given by

$$\begin{aligned}\langle|\mathcal{M}_{fi}|^2\rangle &= \frac{1}{4} \times \left(|\mathcal{M}_{RL\to RL}|^2 + |\mathcal{M}_{RL\to LR}|^2 + |\mathcal{M}_{LR\to RL}|^2 + |\mathcal{M}^2_{LR\to LR}|\right) \\ &= \frac{1}{4} e^4 \left[2(1+\cos\theta)^2 + 2(1-\cos\theta)^2\right] \\ &= e^4(1+\cos^2\theta). \end{aligned} \tag{6.22}$$

The corresponding differential cross section is obtained by substituting the spin-averaged matrix element squared of (6.22) into the general cross section formula of (3.50) with $p_i^* = p_f^* = E$, giving

$$\frac{d\sigma}{d\Omega} = \frac{1}{64\pi^2 s} e^4(1+\cos^2\theta),$$

where the solid angle is defined in terms of the spherical polar angles of the $\mu^-$ as measured in the centre-of-mass frame. Finally, when written in terms of the dimensionless coupling constant $\alpha = e^2/(4\pi)$, the $e^+e^- \to \mu^+\mu^-$ differential cross section becomes

$$\frac{d\sigma}{d\Omega} = \frac{\alpha^2}{4s}(1+\cos^2\theta). \tag{6.23}$$

Figure 6.7 shows the predicted $(1+\cos^2\theta)$ angular distribution of the $e^+e^- \to \mu^+\mu^-$ differential cross section broken down into the contributions from the different helicity combinations. The distribution is forward–backward symmetric, meaning that equal numbers of $\mu^-$ are produced in the forward hemisphere ($\cos\theta > 0$) as in the backwards hemisphere ($\cos\theta < 0$). This symmetry is a direct consequence of the parity conserving nature of the QED interaction, as explained in Chapter 11.

The right-hand plot of Figure 6.7 shows the measured $e^+e^- \to \mu^+\mu^-$ differential cross section at $\sqrt{s} = 34.4\,\text{GeV}$ from the JADE experiment, which operated between 1979 and 1986 at the PETRA $e^+e^-$ collider at the DESY laboratory in Hamburg. The $(1+\cos^2\theta)$ nature of the dominant QED contribution is apparent. However, the interpretation of these data is complicated the presence of electroweak corrections arising from the interference between the QED amplitude and that from the Feynman diagram involving the exchange of a Z boson (see Chapter 15). This results in a relatively small forward–backward asymmetry in the differential cross section.

The total $e^+e^- \to \mu^+\mu^-$ cross section is obtained by integrating (6.23) over the full solid angle range. Writing $d\Omega = d\phi\, d(\cos\theta)$, the solid angle integral is simply

$$\int (1+\cos^2\theta)\, d\Omega = 2\pi \int_{-1}^{+1} (1+\cos^2\theta)\, d(\cos\theta) = \frac{16\pi}{3}.$$

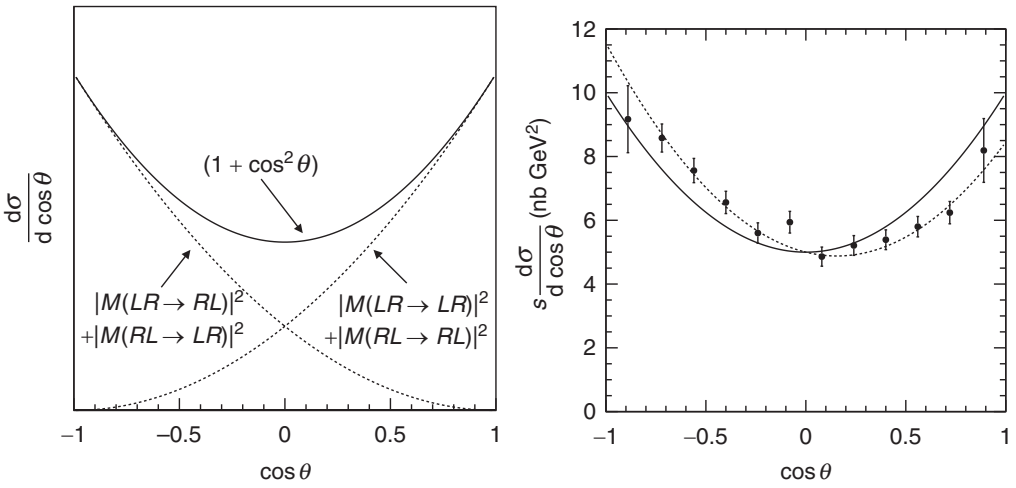


Fig. 6.7 (left) The QED prediction for the distribution of $\cos\theta$ in $e^+e^- \to \mu^+\mu^-$ annihilation, where $\theta$ is the angle of the outgoing $\mu^-$ with respect to the incoming $e^-$ direction. (right) The measured $e^+e^- \to \mu^+\mu^-$ differential cross section at $\sqrt{s} = 34.4$ GeV from the JADE experiment, adapted from Bartel *et al.* (1985). The solid curve is the lowest-order QED prediction. The dotted curve includes electroweak corrections.

Therefore, the lowest-order prediction for the total $e^+e^- \to \mu^+\mu^-$ cross section is

$$\sigma = \frac{4\pi\alpha^2}{3s}. \tag{6.24}$$

Figure 6.8 shows the experimental measurements of the $e^+e^- \to \mu^+\mu^-$ cross section at centre-of-mass energies of $\sqrt{s} < 40$ GeV. In this case, the electroweak corrections are negligible (the effects of interference with the Z boson exchange diagram average to zero in the solid angle integral) and the lowest-order QED prediction provides an excellent description of the data. This is an impressive result, starting from first principles, it has been possible to calculate an expression for the cross section for electron–positron annihilation which is accurate at the $O(1\%)$ level.

### 6.2.5 Lorentz-invariant form

The spin-averaged matrix element of (6.22) is expressed in terms of the angle $\theta$ as measured in the centre-of-mass frame. However, because the matrix element is Lorentz invariant, it also can be expressed in an explicitly Lorentz-invariant form using four-vector scalar products formed from the four-momenta of the initial- and final-state particles. From the four-momenta defined in (6.7)–(6.10),

$$p_1\cdot p_2 = 2E^2, \quad p_1\cdot p_3 = E^2(1-\cos\theta) \quad \text{and} \quad p_1\cdot p_4 = E^2(1+\cos\theta).$$

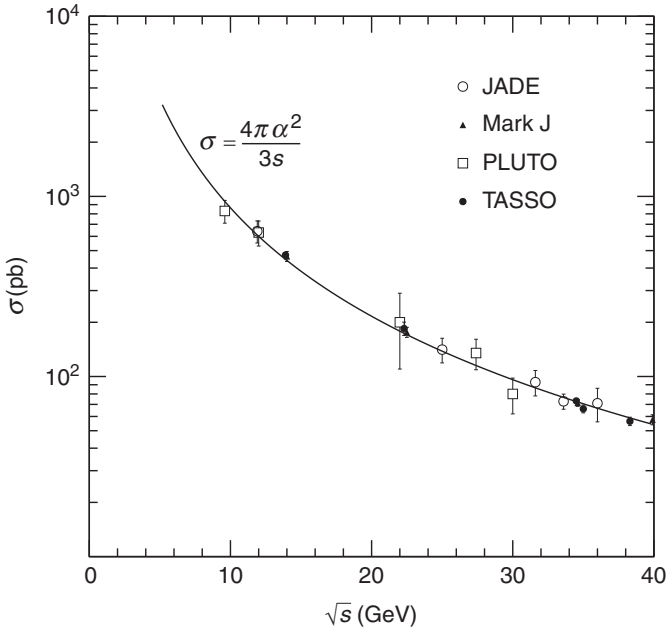


**Fig. 6.8** The measured $e^+e^- \to \mu^+\mu^-$ cross section for $\sqrt{s} < 40$ GeV. The curve shows the lowest-order QED prediction of (6.24).

Hence the spin-averaged matrix element of (6.22) can be written as

$$\langle|\mathcal{M}_{fi}|^2\rangle = 2e^4 \frac{(p_1\cdot p_3)^2 + (p_1\cdot p_4)^2}{(p_1\cdot p_2)^2}. \tag{6.25}$$

The scalar products appearing in (6.25) can be expressed in terms of the Mandelstam variables, where for example

$$s = (p_1 + p_2)^2 = p_1^2 + p_2^2 + 2p_1\cdot p_2 = m_1^2 + m_2^2 + 2p_1\cdot p_2.$$

In the limit, where the masses of the particles can be neglected,

$$s = +2p_1\cdot p_2, \quad t = -2p_1\cdot p_3 \quad \text{and} \quad u = -2p_1\cdot p_4,$$

and therefore (6.25) can be written as

$$\langle|\mathcal{M}_{fi}|^2\rangle = 2e^4\left(\frac{t^2 + u^2}{s^2}\right). \tag{6.26}$$

This expression, which depends only on Lorentz-invariant quantities, is valid in all frames of reference.

## 6.3 Spin in electron–positron annihilation

The four helicity combinations for the process $e^+e^- \to \mu^+\mu^-$ that give non-zero matrix elements are shown in Figure 6.6. In each case, the spins of the two initial-state particles are aligned, as are the spins of the two final-state particles. Defining the $z$-axis to be in the direction of the incoming electron beam, the $z$-component the combined spin of the $e^+$ and $e^-$ is therefore either $+1$ or $-1$, implying that the non-zero matrix elements correspond to the cases where the electron and positron collide in a state of total spin-1. Therefore, the spin state for the *RL* helicity combination can be identified as $|S, S_z\rangle = |1, +1\rangle$ and that for the *LR* combinations as $|1, -1\rangle$. Similarly, the helicity combinations of the $\mu^+\mu^-$ system correspond to spin states of $|1, \pm 1\rangle_\theta$ measured with respect to the axis in the direction of $\mu^-$, as indicated in Figure 6.9.

The angular dependence of the matrix elements for each helicity combination can be understood in terms of these spin states. The operator corresponding to the component of spin along an axis defined by the unit vector $\mathbf{n}$ at an angle $\theta$ to the $z$-axis is $\hat{S}_n = \frac{1}{2}\mathbf{n}\cdot\boldsymbol{\sigma}$. Using this operator, it is possible to express the spin states of the $\mu^+\mu^-$ system in terms of the eigenstates of $\hat{S}_z$ (see Problem 6.6). For example, the spin wavefunction of the *RL* helicity combination of the $\mu^+\mu^-$ final state, $|1, +1\rangle_\theta$, can be expressed as

$$|1, +1\rangle_\theta = \tfrac{1}{2}(1 - \cos\theta)\,|1, -1\rangle + \tfrac{1}{\sqrt{2}}\sin\theta\,|1, 0\rangle + \tfrac{1}{2}(1 + \cos\theta)\,|1, +1\rangle.$$

The angular distributions of matrix elements of (6.20) and (6.21) can be understood in terms of the inner products of the spin states of initial-state $e^+e^-$ system and the

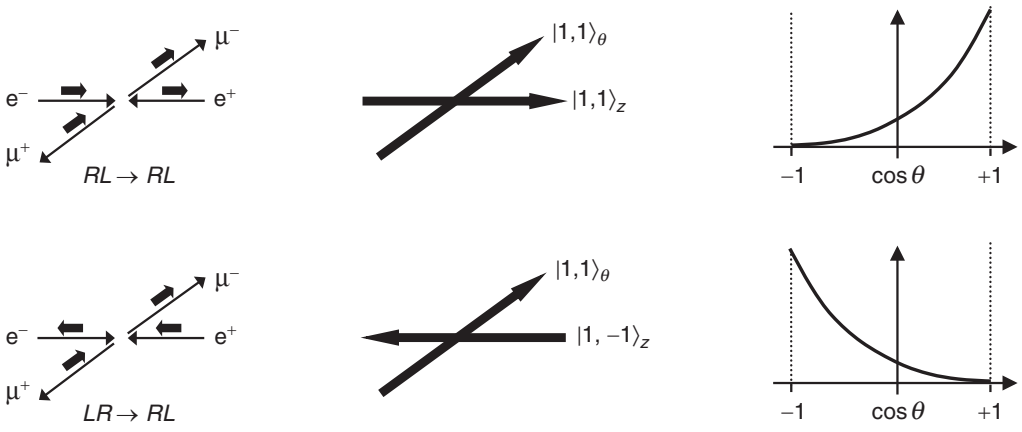


Fig. 6.9 The orientations of the spin-1 system in the $RL \to RL$ and $LR \to RL$ helicity combinations and the angular dependence of the corresponding matrix element in the limit where $E \gg m$.

final-state $\mu^+\mu^-$ system. For example,

$$\mathcal{M}_{RL\to RL} \propto \langle 1,+1|1,+1\rangle_\theta = \tfrac{1}{2}(1+\cos\theta)$$
$$\mathcal{M}_{LR\to RL} \propto \langle 1,-1|1,+1\rangle_\theta = \tfrac{1}{2}(1-\cos\theta).$$

Hence, in the limit $E \gg m$, the spin combinations that give non-zero matrix elements correspond to states of total spin-1 with the spin vector pointing along the direction of the particles motion and the resulting angular distributions can be understood in terms of the quantum mechanics of spin-1. This is consistent with the notion that an interaction of the form $\bar{\phi}\gamma^\mu\psi$ corresponds to the exchange of a spin-1 particle, in this case the photon.

## 6.4 Chirality

In the limit $E \gg m$ only four out of the sixteen possible helicity combinations for the process $e^+e^- \to e^+e^-$ give non-zero matrix elements. This does not happen by chance, but reflects the underlying *chiral* structure of QED. The property of chirality is an important concept in the Standard Model. Chirality is introduced by defining the $\gamma^5$-matrix as

$$\gamma^5 \equiv i\gamma^0\gamma^1\gamma^2\gamma^3 = \begin{pmatrix} 0 & 0 & 1 & 0 \\ 0 & 0 & 0 & 1 \\ 1 & 0 & 0 & 0 \\ 0 & 1 & 0 & 0 \end{pmatrix} = \begin{pmatrix} 0 & I \\ I & 0 \end{pmatrix}. \tag{6.27}$$

The significance of the $\gamma^5$-matrix, whilst not immediately obvious, follows from its mathematical properties and the nature of its eigenstates. The properties of the $\gamma^5$-matrix can be derived (see Problem 6.1) from the commutation and Hermiticity relations of the $\gamma$-matrices given in (4.33) and (4.34), leading to

$$(\gamma^5)^2 = 1, \tag{6.28}$$
$$\gamma^{5\dagger} = \gamma^5, \tag{6.29}$$
$$\gamma^5\gamma^\mu = -\gamma^\mu\gamma^5. \tag{6.30}$$

In the limit $E \gg m$, and only in this limit, the helicity eigenstates of (6.11) are also eigenstates of the $\gamma^5$-matrix with eigenvalues

$$\gamma^5 u_\uparrow = +u_\uparrow, \quad \gamma^5 u_\downarrow = -u_\downarrow, \quad \gamma^5 v_\uparrow = -v_\uparrow \quad \text{and} \quad \gamma^5 v_\downarrow = +v_\downarrow.$$

In general, the eigenstates of the $\gamma^5$-matrix are defined as left- and right-handed *chiral* states (denoted with subscripts $R, L$ to distinguish them from the general helicity eigenstates $\uparrow, \downarrow$) such that

$$\begin{aligned} \gamma^5 u_R &= +u_R \quad \text{and} \quad \gamma^5 u_L = -u_L, \\ \gamma^5 v_R &= -v_R \quad \text{and} \quad \gamma^5 v_L = +v_L. \end{aligned} \tag{6.31}$$

With this convention, when $E \gg m$ the chiral eigenstates are the same as the helicity eigenstates for both particle and antiparticle spinors, for example $u_\uparrow \to u_R$ and $v_\downarrow \to v_L$. Hence, *in general*, the solutions to the Dirac equation which are also eigenstates of $\gamma^5$ are identical to the massless helicity eigenstates of (6.11),

$$u_R \equiv N \begin{pmatrix} c \\ se^{i\phi} \\ c \\ se^{i\phi} \end{pmatrix}, \; u_L \equiv N \begin{pmatrix} -s \\ ce^{i\phi} \\ s \\ -ce^{i\phi} \end{pmatrix}, \; v_R \equiv N \begin{pmatrix} s \\ -ce^{i\phi} \\ -s \\ ce^{i\phi} \end{pmatrix} \text{ and } v_L \equiv N \begin{pmatrix} c \\ se^{i\phi} \\ c \\ se^{i\phi} \end{pmatrix}, \tag{6.32}$$

where the normalisation is given by $N = \sqrt{E+m}$. Unlike helicity, there is no simple physical interpretation of the property of chirality, it is nevertheless an integral part of the structure of the Standard Model.

### Chiral projection operators

Any Dirac spinor can be decomposed into left- and right-handed chiral components using the chiral projection operators, $P_L$ and $P_R$, defined by

$$\begin{aligned} P_R &= \tfrac{1}{2}(1+\gamma^5), \\ P_L &= \tfrac{1}{2}(1-\gamma^5). \end{aligned} \tag{6.33}$$

Using the properties of the $\gamma^5$-matrix, it is straightforward to show that $P_R$ and $P_L$ satisfy the required algebra of quantum mechanical projection operators, namely,

$$P_R + P_L = 1, \quad P_R P_R = P_R, \quad P_L P_L = P_L \quad \text{and} \quad P_L P_R = 0.$$

In the Dirac–Pauli representation

$$P_R = \tfrac{1}{2}\begin{pmatrix} 1 & 0 & 1 & 0 \\ 0 & 1 & 0 & 1 \\ 1 & 0 & 1 & 0 \\ 0 & 1 & 0 & 1 \end{pmatrix} \text{ and } P_L = \tfrac{1}{2}\begin{pmatrix} 1 & 0 & -1 & 0 \\ 0 & 1 & 0 & -1 \\ -1 & 0 & 1 & 0 \\ 0 & -1 & 0 & 1 \end{pmatrix}. \tag{6.34}$$

From the definitions of (6.31), it immediately follows that the right-handed chiral projection operator has the properties

$$P_R u_R = u_R, \quad P_R u_L = 0, \quad P_R v_R = 0 \quad \text{and} \quad P_R v_L = v_L.$$

Hence $P_R$ projects out *right-handed* chiral *particle* states and *left-handed* chiral *antiparticle* states. Similarly, for the left-handed chiral projection operator,

$$P_L u_R = 0, \quad P_L u_L = u_L, \quad P_L v_R = v_R \quad \text{and} \quad P_L v_L = 0.$$

Since $P_R$ and $P_L$ project out chiral states, any spinor $u$ can be decomposed into left- and right-handed chiral components with

$$u = a_R\, u_R + a_L\, u_L = \tfrac{1}{2}(1+\gamma^5)u + \tfrac{1}{2}(1-\gamma^5)u,$$

where $a_R$ and $a_L$ are complex coefficients and $u_R$ and $u_L$ are right- and left-handed chiral eigenstates.

### 6.4.1 Chirality in QED

In QED, the fundamental interaction between a fermion and a photon is expressed as a four-vector current $iQ_f e\overline{\psi}\gamma^\mu\phi$, formed from the Dirac spinors $\psi$ and $\phi$. Any four-vector current can be decomposed into contributions from left- and right-handed chiral states using the chiral projection operators defined in (6.33). For example, in the case of QED,

$$\begin{aligned}\overline{\psi}\gamma^\mu\phi &= (a_R^*\overline{\psi}_R + a_L^*\overline{\psi}_L)\gamma^\mu(b_R\phi_R + b_L\phi_L)\\ &= a_R^* b_R\overline{\psi}_R\gamma^\mu\phi_R + a_R^* b_L\overline{\psi}_R\gamma^\mu\phi_L + a_L^* b_R\overline{\psi}_L\gamma^\mu\phi_R + a_L^* b_L\overline{\psi}_L\gamma^\mu\phi_L,\end{aligned} \tag{6.35}$$

where the coefficients, $a$ and $b$, will depend on the spinors being considered. The form of the QED interaction means that two of the chiral currents in (6.35) are always zero. For example, consider the term $\overline{u}_L(p)\gamma^\mu u_R(p')$. The action of $P_R$ on a right-handed chiral spinor leaves the spinor unchanged,

$$u_R(p') = P_R u_R(p'). \tag{6.36}$$

Therefore $P_R$ can always be inserted in front of right-handed chiral particle state without changing the expression in which it appears. The equivalent relation for the left-handed adjoint spinor is

$$\begin{aligned}\overline{u}_L(p) \equiv [u_L(p)]^\dagger\gamma^0 &= [P_L u_L(p)]^\dagger\gamma^0 = [\tfrac{1}{2}(1-\gamma^5)u_L(p)]^\dagger\gamma^0\\ &= [u_L(p)]^\dagger\tfrac{1}{2}(1-\gamma^5)\gamma^0 && \text{(using } \gamma^5 = \gamma^{5\dagger}\text{)}\\ &= [u_L(p)]^\dagger\gamma^0\tfrac{1}{2}(1+\gamma^5) && \text{(using } \gamma^0\gamma^5 = -\gamma^5\gamma^0\text{)}\\ &= \overline{u}_L(p)P_R.\end{aligned}$$

From this it follows that

$$\overline{u}_L(p)\gamma^\mu u_R(p') = \overline{u}_L(p)P_R\,\gamma^\mu P_R\, u_R(p'). \tag{6.37}$$

But since $\gamma^5\gamma^\mu = -\gamma^\mu\gamma^5$,

$$P_R\gamma^\mu = \tfrac{1}{2}(1+\gamma^5)\gamma^\mu = \gamma^\mu\tfrac{1}{2}(1-\gamma^5) = \gamma^\mu P_L,$$

and thus (6.37) can be written

$$\overline{u}_L(p)\gamma^\mu u_R(p') = \overline{u}_L(p)\gamma^\mu P_L P_R\, u_R(p') = 0,$$

because $P_L P_R = 0$. Therefore, the $\overline{\psi}\gamma^\mu\phi$ form of the QED interaction, implies that only certain combinations of chiral eigenstates give non-zero matrix elements, and the currents of the form

$$\bar{u}_L\gamma^\mu u_R = \bar{u}_R\gamma^\mu u_L = \bar{v}_L\gamma^\mu v_R = \bar{v}_R\gamma^\mu v_L = \bar{v}_L\gamma^\mu u_L = \bar{v}_R\gamma^\mu u_R \equiv 0$$

are always identically zero.

### 6.4.2 Helicity and chirality

It is important not to confuse the concepts of helicity and chirality. Helicity eigenstates are defined by the projection of the spin of a particle onto its direction of motion, whereas the chiral states are the eigenstates of the $\gamma^5$-matrix. The relationship between the helicity eigenstates and the chiral eigenstates can be found by decomposing the general form of the helicity spinors into their chiral components. For example, the right-handed helicity particle spinor of (4.65) can be written as

$$u_\uparrow(\mathrm{p},\theta,\phi) = N\begin{pmatrix} c \\ se^{i\phi} \\ \kappa c \\ \kappa s e^{i\phi} \end{pmatrix} \quad \text{with} \quad \kappa = \frac{\mathrm{p}}{E+m} \quad \text{and} \quad N = \sqrt{E+m}.$$

The spinor can be decomposed into its left- and right-handed chiral components by considering the effect of the chiral projection operators,

$$P_R u_\uparrow = \tfrac{1}{2}(1+\kappa)\,N\begin{pmatrix} c \\ se^{i\phi} \\ c \\ se^{i\phi} \end{pmatrix} \quad \text{and} \quad P_L u_\uparrow = \tfrac{1}{2}(1-\kappa)\,N\begin{pmatrix} c \\ se^{i\phi} \\ -c \\ -se^{i\phi} \end{pmatrix}.$$

Therefore, the right-handed helicity spinor, expressed in terms of its chiral components, is

$$\begin{aligned} u_\uparrow(\mathrm{p},\theta,\phi) &= \tfrac{1}{2}(1+\kappa)\,N\begin{pmatrix} c \\ se^{i\phi} \\ c \\ se^{i\phi} \end{pmatrix} + \tfrac{1}{2}(1-\kappa)\,N\begin{pmatrix} c \\ se^{i\phi} \\ -c \\ -se^{i\phi} \end{pmatrix} \\ &\propto \tfrac{1}{2}(1+\kappa)\,u_R + \tfrac{1}{2}(1-\kappa)\,u_L, \end{aligned} \tag{6.38}$$

where $u_R$ and $u_L$ are chiral eigenstates with $\gamma^5 u_R = +u_R$ and $\gamma^5 u_L = -u_L$. From (6.38) it is clear that it is only in the limit where $E \gg m$ (when $\kappa \to 1$) that the helicity eigenstates are equivalent to the chiral eigenstates. Because only certain combinations of chiral states give non-zero contributions to the QED matrix element, in the ultra-relativistic limit only the corresponding helicity combinations

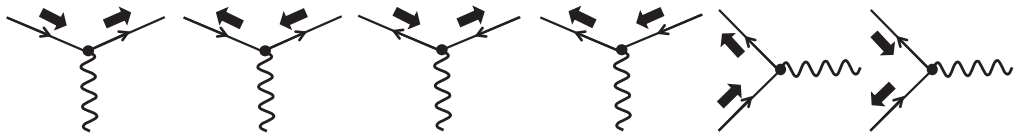

Fig. 6.10 The helicity combinations at the QED vertex which give non-zero four-vector currents in the limit $E \gg m$.

contribute to the QED interaction. The chiral nature of the QED interaction therefore explains the previous observation that only four of the sixteen possible helicity combinations contribute to the $e^+e^- \to \mu^+\mu^-$ annihilation process at high energies.

The correspondence between the helicity and chiral eigenstates in the ultra-relativistic limit implies that for $E \gg m$, the four-vector currents written in terms of the helicity states,

$$\bar{u}_\downarrow \gamma^\mu u_\uparrow = \bar{u}_\uparrow \gamma^\mu u_\downarrow = \bar{v}_\downarrow \gamma^\mu v_\uparrow = \bar{v}_\uparrow \gamma^\mu v_\downarrow = \bar{v}_\downarrow \gamma^\mu u_\downarrow = \bar{v}_\uparrow \gamma^\mu u_\uparrow = 0,$$

are all zero. Therefore in the high-energy QED processes, only the helicity combinations shown in Figure 6.10 give non-zero currents. Consequently, the helicity of the particle leaving the QED vertex is that same as that entering it and helicity is effectively "conserved" in *high-energy* interactions.

## 6.5 *Trace techniques

In the calculation of the $e^+e^- \to \mu^+\mu^-$ cross section described above, the individual matrix elements were calculated for each helicity combination using the explicit representations of the spinors and the $\gamma$-matrices. The resulting squares of the matrix elements were then summed and averaged. This approach is relatively simple and exposes the underlying physics of the interaction. For these reasons, the majority of the calculations that follow will adopt the helicity amplitude approach. In the limit where the masses of the particles can be neglected, these calculations are relatively straightforward as they involve only a limited number of helicity combinations. However, when the particle masses can not be neglected, it is necessary to consider all possible spin combinations. In this case, calculating the individual helicity amplitudes is not particularly efficient (although it is well suited to computational calculations). For more complicated processes, analytic solutions are usually most easily obtained using a powerful technique based on the traces of matrices and the completeness relations for Dirac spinors.

### 6.5.1 Completeness relations

Sums over the spin states of the initial- and final-state particles can be calculated using the completeness relations satisfied by Dirac spinors. The completeness

relations are defined by the sum over the two possible spin states of the tensor formed from the product of a spinor with its adjoint spinor,

$$\sum_{s=1}^{2} u_s(p)\overline{u}_s(p),$$

where the sum is for two orthogonal spin states. The sum can be performed using the helicity basis or the spinors $u_1$ and $u_2$, both of which form a complete set of states. Here it is most convenient to work with the spinors $u_1(p)$ and $u_2(p)$, in which case the completeness relation is

$$\sum_{s=1}^{2} u_s(p)\overline{u}_s(p) \equiv u_1(p)\overline{u}_1(p) + u_2(p)\overline{u}_2(p).$$

In the Dirac–Pauli representation, the spinors $u_1$ and $u_2$ can be written as

$$u_s(p) = \sqrt{E+m}\begin{pmatrix} \phi_s \\ \frac{\boldsymbol{\sigma}\cdot\mathbf{p}}{E+m}\phi_s \end{pmatrix} \quad \text{with} \quad \phi_1 = \begin{pmatrix} 1 \\ 0 \end{pmatrix} \quad \text{and} \quad \phi_2 = \begin{pmatrix} 0 \\ 1 \end{pmatrix}.$$

Using $(\boldsymbol{\sigma}\cdot\mathbf{p})^\dagger = \boldsymbol{\sigma}\cdot\mathbf{p}$, the adjoint spinor can be written

$$\overline{u}_s = u_s^\dagger\gamma^0 = \sqrt{E+m}\begin{pmatrix} \phi_s^T & \phi_s^T\frac{(\boldsymbol{\sigma}\cdot\mathbf{p})^\dagger}{E+m} \end{pmatrix}\begin{pmatrix} I & 0 \\ 0 & -I \end{pmatrix} = \sqrt{E+m}\begin{pmatrix} \phi_s^T & -\phi_s^T\frac{(\boldsymbol{\sigma}\cdot\mathbf{p})}{E+m} \end{pmatrix},$$

where $I$ is the $2\times2$ identity matrix. Hence the completeness relation can be written

$$\sum_{s=1}^{2} u_s(p)\overline{u}_s(p) = (E+m)\sum_{s=1}^{2}\begin{pmatrix} \phi_s\phi_s^T & -\frac{\boldsymbol{\sigma}\cdot\mathbf{p}}{E+m}\phi_s\phi_s^T \\ \frac{\boldsymbol{\sigma}\cdot\mathbf{p}}{E+m}\phi_s\phi_s^T & -\frac{(\boldsymbol{\sigma}\cdot\mathbf{p})^2}{(E+m)^2}\phi_s\phi_s^T \end{pmatrix},$$

which using

$$\sum_{s=1}^{2}\phi_s\phi_s^T = \begin{pmatrix} 1 & 0 \\ 0 & 1 \end{pmatrix} \quad \text{and} \quad (\boldsymbol{\sigma}\cdot\mathbf{p})^2 = \mathbf{p}^2 = (E+m)(E-m),$$

gives

$$\sum_{s=1}^{2} u_s(p)\overline{u}_s(p) = \begin{pmatrix} (E+m)I & -\boldsymbol{\sigma}\cdot\mathbf{p} \\ \boldsymbol{\sigma}\cdot\mathbf{p} & (-E+m)I \end{pmatrix}. \tag{6.39}$$

Equation (6.39) can be written in terms of the $\gamma$-matrices as

$$\sum_{s=1}^{2} u_s\overline{u}_s = (\gamma^\mu p_\mu + mI) = \not{p} + m, \tag{6.40}$$

where the "slash" notation is shorthand for $\not{p} \equiv \gamma^\mu p_\mu = E\gamma^0 - p_x\gamma^1 - p_y\gamma^2 - p_z\gamma^3$. Repeating the above derivation, it is straightforward to show that the antiparticle spinors satisfy the completeness relation,

$$\sum_{r=1}^{2} v_r \bar{v}_r = (\gamma^\mu p_\mu - mI) = \not{p} - m, \tag{6.41}$$

where the mass term enters with a different sign compared to the equivalent expression for particle spinors.

### 6.5.2 Spin sums and the trace formalism

The QED, QCD and weak interaction vertex factors all can be written in the form $\bar{u}(p)\,\Gamma\,u(p')$, where $\Gamma$ is a $4 \times 4$ matrix constructed out of one or more Dirac $\gamma$-matrices. In index notation, this product of spinors and $\gamma$-matrices can be written

$$\bar{u}(p)\,\Gamma\,u(p') = \bar{u}(p)_j\,\Gamma_{ji}\,u(p')_i,$$

where the indices label the components and summation over repeated indices is implied. It should be noted that $\bar{u}(p)\,\Gamma\,u(p')$ is simply a (complex) number.[1] For the QED vertex $\Gamma = \gamma^\mu$ and the matrix element for the process $e^+e^- \to \mu^+\mu^-$ is given by (6.3),

$$\begin{aligned}\mathcal{M}_{fi} &= -\frac{e^2}{q^2}\left[\bar{v}(p_2)\gamma^\mu u(p_1)\right] g_{\mu\nu}\left[\bar{u}(p_3)\gamma^\nu v(p_4)\right] \\ &= -\frac{e^2}{q^2}\Big[\bar{v}(p_2)\gamma^\mu u(p_1)\Big]\Big[\bar{u}(p_3)\gamma_\mu v(p_4)\Big],\end{aligned} \tag{6.42}$$

where summation over the index $\mu$ is implied. The matrix element squared $|\mathcal{M}_{fi}|^2$ is the product of $\mathcal{M}_{fi}$ and $\mathcal{M}_{fi}^\dagger$, with

$$\mathcal{M}_{fi}^\dagger = \frac{e^2}{q^2}\left[\bar{v}(p_2)\gamma^\nu u(p_1)\right]^\dagger\left[\bar{u}(p_3)\gamma_\nu v(p_4)\right]^\dagger,$$

where the index $\nu$ has been used for this summation to avoid confusion with the index $\mu$ in the expression for $\mathcal{M}_{fi}$ given in (6.42). Because the components of the

[1] If this is not immediately obvious, consider the $2 \times 2$ case of $\mathbf{c}^{\mathrm{T}}\mathbf{B}\mathbf{a}$, where the equivalent product can be written as

$$\begin{aligned}(c_1, c_2)\begin{pmatrix} B_{11} & B_{12} \\ B_{22} & B_{22}\end{pmatrix}\begin{pmatrix} a_1 \\ a_2\end{pmatrix} &= c_1B_{11}a_1 + c_1B_{12}a_2 + c_2B_{21}a_1 + c_2B_{22} \\ &= c_jB_{ji}a_i,\end{aligned}$$

which is just the sum over the product of the components of $\mathbf{a}$, $\mathbf{c}$ and $\mathbf{B}$.

currents are simply numbers, the order in which they are written does not matter. Hence $|\mathcal{M}_{fi}|^2 = \mathcal{M}_{fi}\mathcal{M}_{fi}^\dagger$ can be written

$$|\mathcal{M}_{fi}|^2 = \frac{e^4}{q^4}\left[\overline{v}(p_2)\gamma^\mu u(p_1)\right]\left[\overline{v}(p_2)\gamma^\nu u(p_1)\right]^\dagger \times \left[\overline{u}(p_3)\gamma_\mu v(p_4)\right]\left[\overline{u}(p_3)\gamma_\nu v(p_4)\right]^\dagger .$$

The spin-averaged matrix element squared can therefore be written

$$\begin{aligned}\langle|\mathcal{M}_{fi}|^2\rangle &= \frac{1}{4}\sum_{\text{spins}}|\mathcal{M}_{fi}|^2 \\ &= \frac{e^4}{4q^4}\sum_{s,r}\left[\overline{v}^r(p_2)\gamma^\mu u^s(p_1)\right]\left[\overline{v}^r(p_2)\gamma^\nu u^s(p_1)\right]^\dagger \\ &\quad\times\sum_{s',r'}\left[\overline{u}^{s'}(p_3)\gamma_\mu v^{r'}(p_4)\right],\left[\overline{u}^{s'}(p_3)\gamma_\nu v^{r'}(p_4)\right]^\dagger ,\end{aligned} \tag{6.43}$$

where $s$, $s'$, $r$ and $r'$ are the labels for the two possible spin states (or equivalently helicity states) of the four spinors. In this way, the calculation of the spin-averaged matrix element squared has been reduced to the product of two terms of the form

$$\sum_{\text{spins}}\left[\overline{\psi}\Gamma_1\phi\right]\left[\overline{\psi}\Gamma_2\phi\right]^\dagger , \tag{6.44}$$

where $\Gamma_1$ and $\Gamma_2$ are two $4\times4$ matrices, which for this QED process are $\Gamma_1 = \gamma^\mu$ and $\Gamma_2 = \gamma^\nu$. Equation (6.44) can be simplified by writing

$$\left[\overline{\psi}\Gamma\phi\right]^\dagger = \left[\psi^\dagger\gamma^0\Gamma\phi\right]^\dagger = \phi^\dagger\Gamma^\dagger\gamma^{0\dagger}\psi = \phi^\dagger\gamma^0\gamma^0\Gamma^\dagger\gamma^0\psi = \overline{\phi}\gamma^0\Gamma^\dagger\gamma^0\psi,$$

and hence

$$\left[\overline{\psi}\Gamma\phi\right]^\dagger \equiv \overline{\phi}\,\overline{\Gamma}\psi \quad \text{with} \quad \overline{\Gamma} = \gamma^0\Gamma^\dagger\gamma^0.$$

From the properties of the $\gamma$-matrices given (4.33) and (4.34), it can be seen that $\gamma^0\gamma^{\mu\dagger}\gamma^0 = \gamma^\mu$ for all $\mu$. Hence for the QED vertex, with $\Gamma = \gamma^\mu$,

$$\overline{\Gamma} = \gamma^0\gamma^{\mu\dagger}\gamma^0 = \gamma^\mu = \Gamma.$$

Although not shown explicitly, it should be noted that $\overline{\Gamma} = \Gamma$ also holds for the QCD and weak interaction vertices. Hence for all of the Standard Model interactions,

$$\left[\overline{\psi}\Gamma\phi\right]^\dagger \equiv \overline{\phi}\,\Gamma\psi. \tag{6.45}$$

Using (6.45), the spin-averaged matrix element squared for the process $e^+e^- \to \mu^+\mu^-$ of (6.43) can be written

$$\sum_{\text{spins}} |\mathcal{M}_{fi}|^2 = \frac{e^4}{q^4} \sum_{s,r} \left[\overline{v}^r(p_2)\gamma^\mu u^s(p_1)\right]\left[\overline{u}^s(p_1)\gamma^\nu v^r(p_2)\right] \times \sum_{s',r'} \left[\overline{u}^{s'}(p_3)\gamma_\mu v^{r'}(p_4)\right]\left[\overline{v}^{r'}(p_4)\gamma_\nu u^{s'}(p_3)\right]. \tag{6.46}$$

Denoting the part of (6.46) involving the initial-state $e^+$ and $e^-$ spinors by the tensor $\mathcal{L}^{\mu\nu}_{(e)}$ and writing the matrix multiplication in index form gives

$$\mathcal{L}^{\mu\nu}_{(e)} = \sum_{s,r=1}^{2} \overline{v}^r_j(p_2)\gamma^\mu_{ji} u^s_i(p_1)\ \overline{u}^s_n(p_1)\gamma^\nu_{nm} v^r_m(p_2)\,. \tag{6.47}$$

Since all the quantities in (6.47) are just numbers, with the indices keeping track of the matrix multiplication, this can be written as

$$\mathcal{L}^{\mu\nu}_{(e)} = \left[\sum_{r=1}^{2} v^r_m(p_2)\overline{v}^r_j(p_2)\right]\left[\sum_{s=1}^{2} u^s_i(p_1)\overline{u}^s_n(p_1)\right]\gamma^\mu_{ji}\gamma^\nu_{nm}\,. \tag{6.48}$$

Using the completeness relations of (6.40), the electron tensor of (6.48) becomes

$$\mathcal{L}^{\mu\nu}_{(e)} = (\not{p}_2 - m)_{mj}(\not{p}_1 + m)_{in}\gamma^\mu_{ji}\gamma^\nu_{nm}, \tag{6.49}$$

where $(\not{p}_2 - m)_{mj}$ is the $(mj)$th element of the $4\times 4$ matrix $(\not{p}_2 - mI)$. Equation (6.49) can be put back into normal matrix multiplication order to give

$$\begin{aligned}\mathcal{L}^{\mu\nu}_{(e)} &= (\not{p}_2 - m)_{mj}\gamma^\mu_{ji}(\not{p}_1 + m)_{in}\gamma^\nu_{nm} \\ &= \left[(\not{p}_2 - m)\gamma^\mu(\not{p}_1 + m)\gamma^\nu\right]_{mm} \\ &= \text{Tr}\left([\not{p}_2 - m]\gamma^\mu[\not{p}_1 + m]\gamma^\nu\right).\end{aligned} \tag{6.50}$$

Consequently, the sum over spins of the initial-state particles has been replaced by the calculation of the traces of $4\times 4$ matrices, one for each of the sixteen possible combinations of the indices $\mu$ and $\nu$. The order in which the two $\not{p}$ terms appear in trace calculation of (6.50) follows the order in which the spinors appear in the original four-vector currents; the $\not{p}$ term associated with the adjoint spinor appears first (although traces are unchanged by cycling the elements). In constructing the traces associated with a Feynman diagram it is helpful to remember that the order in which different terms appear can be obtained by following the arrows in the fermion currents in the backwards direction. Writing the sum over the spins of final-state particles of (6.46) as the muon tensor,

$$\mathcal{L}^{(\mu)}_{\mu\nu} = \sum_{s',r'} \left[\overline{u}^{s'}(p_3)\gamma_\mu v^{r'}(p_4)\right]\left[\overline{v}^{r'}(p_4)\gamma_\nu u^{s'}(p_3)\right],$$

and expressing this in terms of a trace, leads to

$$\sum_{\text{spins}} |\mathcal{M}_{fi}|^2 = \frac{e^4}{q^4} \mathcal{L}^{\mu\nu}_{(\text{e})} \mathcal{L}^{(\mu)}_{\mu\nu}$$
$$= \frac{e^4}{q^4} \text{Tr}\left([\not{p}_2 - m]\gamma^\mu[\not{p}_1 + m]\gamma^\nu\right) \times \text{Tr}\left([\not{p}_3 + M]\gamma_\mu[\not{p}_4 - M]\gamma_\nu\right), \tag{6.51}$$

where the masses of the initial- and final-state particles are respectively written as $m$ and $M$.

### 6.5.3 Trace theorems

The calculation of the spin-summed matrix element has been reduced to a problem of calculating traces involving combinations of $\gamma$-matrices. At first sight this appears a daunting task, but fortunately there are a number of algebraic "tricks" which greatly simplify the calculations. Firstly, traces have the properties

$$\text{Tr}\,(A + B) \equiv \text{Tr}\,(A) + \text{Tr}\,(B), \tag{6.52}$$

and are unchanged by cycling the order of the elements

$$\text{Tr}\,(AB \ldots YZ) \equiv \text{Tr}\,(ZAB \ldots Y). \tag{6.53}$$

Secondly, the algebra of the $\gamma$-matrices is defined by the anticommutation relation of (4.33), namely

$$\gamma^\mu\gamma^\nu + \gamma^\nu\gamma^\mu \equiv 2g^{\mu\nu}I, \tag{6.54}$$

where the presence of the $4 \times 4$ identity matrix has been made explicit. Taking the trace of (6.54) gives

$$\text{Tr}\,(\gamma^\mu\gamma^\nu) + \text{Tr}\,(\gamma^\nu\gamma^\mu) = 2g^{\mu\nu}\,\text{Tr}\,(I),$$

which using $\text{Tr}\,(AB) = \text{Tr}\,(BA)$ becomes $\text{Tr}\,(\gamma^\mu\gamma^\nu) = g^{\mu\nu}\,\text{Tr}\,(I)$, and hence

$$\text{Tr}\,(\gamma^\mu\gamma^\nu) = 4g^{\mu\nu}. \tag{6.55}$$

The trace of any odd number of $\gamma$-matrices can be shown to be zero by inserting $\gamma^5\gamma^5 = I$ into the trace. For example, consider the trace of any three $\gamma$-matrices

$$\begin{aligned}
\text{Tr}\,(\gamma^\mu\gamma^\nu\gamma^\rho) &= \text{Tr}\left(\gamma^5\gamma^5\gamma^\mu\gamma^\nu\gamma^\rho\right) \\
&= \text{Tr}\left(\gamma^5\gamma^\mu\gamma^\nu\gamma^\rho\gamma^5\right) && \text{(traces are cyclical)} \\
&= -\text{Tr}\left(\gamma^5\gamma^5\gamma^\mu\gamma^\nu\gamma^\rho\right) && \text{(since } \gamma^5\gamma^\mu = -\gamma^\mu\gamma^5\text{)}
\end{aligned}$$

where the last line follows from commuting $\gamma^5$ through the three $\gamma$-matrices, each time introducing a factor of $-1$. Hence $\mathrm{Tr}\,(\gamma^\mu\gamma^\nu\gamma^\rho) = -\,\mathrm{Tr}\,(\gamma^\mu\gamma^\nu\gamma^\rho)$, which can only be true if

$$\mathrm{Tr}\,(\gamma^\mu\gamma^\nu\gamma^\rho) = 0. \tag{6.56}$$

The same argument can be applied to show that the trace of *any* odd number of $\gamma$-matrices is zero.

Finally, the trace of four $\gamma$-matrices can be obtained from (6.54) which allows $\gamma^a\gamma^b$ to be written as $2g^{ab} - \gamma^b\gamma^a$ and repeated application of this identity gives

$$\begin{aligned}
\gamma^\mu\gamma^\nu\gamma^\rho\gamma^\sigma &= 2g^{\mu\nu}\gamma^\rho\gamma^\sigma - \gamma^\nu\gamma^\mu\gamma^\rho\gamma^\sigma \\
&= 2g^{\mu\nu}\gamma^\rho\gamma^\sigma - 2g^{\mu\rho}\gamma^\nu\gamma^\sigma + \gamma^\nu\gamma^\rho\gamma^\mu\gamma^\sigma \\
&= 2g^{\mu\nu}\gamma^\rho\gamma^\sigma - 2g^{\mu\rho}\gamma^\nu\gamma^\sigma + 2g^{\mu\sigma}\gamma^\nu\gamma^\rho - \gamma^\nu\gamma^\rho\gamma^\sigma\gamma^\mu \\
\Rightarrow \quad \gamma^\mu\gamma^\nu\gamma^\rho\gamma^\sigma + \gamma^\nu\gamma^\rho\gamma^\sigma\gamma^\mu &= 2g^{\mu\nu}\gamma^\rho\gamma^\sigma - 2g^{\mu\rho}\gamma^\nu\gamma^\sigma + 2g^{\mu\sigma}\gamma^\nu\gamma^\rho. \qquad (6.57)
\end{aligned}$$

Taking the trace of both sides of (6.57) and using the cyclic property of traces

$$2\mathrm{Tr}\,(\gamma^\mu\gamma^\nu\gamma^\rho\gamma^\sigma) = 2g^{\mu\nu}\,\mathrm{Tr}\,(\gamma^\rho\gamma^\sigma) - 2g^{\mu\rho}\,\mathrm{Tr}\,(\gamma^\nu\gamma^\sigma) + 2g^{\mu\sigma}\,\mathrm{Tr}\,(\gamma^\nu\gamma^\rho),$$

and using (6.55) for the trace of two $\gamma$-matrices gives the identity

$$\mathrm{Tr}\,(\gamma^\mu\gamma^\nu\gamma^\rho\gamma^\sigma) = 4g^{\mu\nu}g^{\rho\sigma} - 4g^{\mu\rho}g^{\nu\sigma} + 4g^{\mu\sigma}g^{\nu\rho}. \tag{6.58}$$

The full set of trace theorems, including those involving $\gamma^5 = i\gamma^0\gamma^1\gamma^2\gamma^3$, are:

(a) $\mathrm{Tr}\,(I) = 4$;
(b) the trace of any odd number of $\gamma$-matrices is zero;
(c) $\mathrm{Tr}\,(\gamma^\mu\gamma^\nu) = 4g^{\mu\nu}$;
(d) $\mathrm{Tr}\,(\gamma^\mu\gamma^\nu\gamma^\rho\gamma^\sigma) = 4g^{\mu\nu}g^{\rho\sigma} - 4g^{\mu\rho}g^{\nu\sigma} + 4g^{\mu\sigma}g^{\nu\rho}$;
(e) the trace of $\gamma^5$ multiplied by an odd number of $\gamma$-matrices is zero;
(f) $\mathrm{Tr}\left(\gamma^5\right) = 0$;
(g) $\mathrm{Tr}\left(\gamma^5\gamma^\mu\gamma^\nu\right) = 0$; and
(h) $\mathrm{Tr}\left(\gamma^5\gamma^\mu\gamma^\nu\gamma^\rho\gamma^\sigma\right) = 4i\varepsilon^{\mu\nu\rho\sigma}$, where $\varepsilon^{\mu\nu\rho\sigma}$ is antisymmetric under the interchange of any two indices.

Armed with these trace theorems, expressions such as that of (6.51) can be evaluated relatively easily; it is worth going through one example of a matrix element calculation using the trace methodology in gory detail.

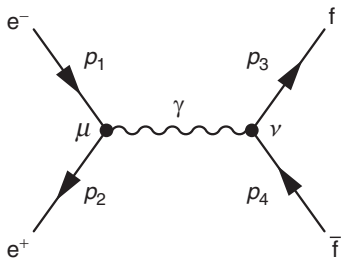


Fig. 6.11 The lowest-order QED Feynman diagram for $e^+e^- \to f\bar{f}$.

### 6.5.4 Electron–positron annihilation revisited

Consider the process $e^+e^- \to f\bar{f}$, shown in Figure 6.11, where f represents any of the fundamental spin-half charged fermions. In the limit where the electron mass can be neglected, but the masses of the final-state fermions cannot, the spin-averaged matrix element squared is given by (6.51) with $m = 0$ and $M = m_f$,

$$\langle|\mathcal{M}_{fi}|^2\rangle = \frac{1}{4}\sum_{\text{spins}}|\mathcal{M}_{fi}|^2 = \frac{Q_f^2 e^4}{4q^4}\,\text{Tr}\left(\not{p}_2\gamma^\mu\not{p}_1\gamma^\nu\right)\,\text{Tr}\left([\not{p}_3 + m_f]\gamma_\mu[\not{p}_4 - m_f]\gamma_\nu\right). \tag{6.59}$$

This can be evaluated by writing $\not{p}_1 = \gamma^\sigma p_{1\sigma}$ and $\not{p}_2 = \gamma^\rho p_{2\rho}$, in which case the first trace in (6.59) can be written as

$$\begin{aligned}\text{Tr}\left(\not{p}_2\gamma^\mu\not{p}_1\gamma^\nu\right) &= p_{2\rho}p_{1\sigma}\text{Tr}\left(\gamma^\rho\gamma^\mu\gamma^\sigma\gamma^\nu\right)\\ &= 4p_{2\rho}p_{1\sigma}(g^{\rho\mu}g^{\sigma\nu} - g^{\rho\sigma}g^{\mu\nu} + g^{\rho\nu}g^{\mu\sigma})\\ &= 4p_2^\mu p_1^\nu - 4g^{\mu\nu}(p_1\cdot p_2) + 4p_2^\nu p_1^\mu.\end{aligned}$$

Since the trace of an odd number of $\gamma$-matrices is zero and $\text{Tr}(A+B) = \text{Tr}(A) + \text{Tr}(B)$, the second trace in (6.59) can be written

$$\text{Tr}\left([\not{p}_3 + m_f]\gamma_\mu[\not{p}_4 - m_f]\gamma_\nu\right) = \text{Tr}\left(\not{p}_3\gamma_\mu\not{p}_4\gamma_\nu\right) - m_f^2\text{Tr}\left(\gamma_\mu\gamma_\nu\right) \tag{6.60}$$

$$= 4p_{3\mu}p_{4\nu} - 4g_{\mu\nu}(p_3\cdot p_4) + 4p_{3\nu}p_{4\mu} - 4m_f^2 g_{\mu\nu}. \tag{6.61}$$

Hence, the spin-averaged matrix element squared is given by

$$\begin{aligned}\langle|\mathcal{M}_{fi}|^2\rangle = 16\frac{Q_f^2 e^4}{4q^4}&\left[p_2^\mu p_1^\nu - g^{\mu\nu}(p_1\cdot p_2) + p_2^\nu p_1^\mu\right]\\ &\times\left[p_{3\mu}p_{4\nu} - g_{\mu\nu}(p_3\cdot p_4) + p_{3\nu}p_{4\mu} - m_f^2 g_{\mu\nu}\right].\end{aligned} \tag{6.62}$$

This expression can be simplified by contracting the indices, where for example

$$g^{\mu\nu}g_{\mu\nu} = 4, \quad p_2^\mu p_1^\nu g_{\mu\nu} = (p_1\cdot p_2) \quad \text{and} \quad p_2^\mu p_1^\nu p_{3\mu}p_{4\nu} = (p_2\cdot p_3)(p_1\cdot p_4).$$

Thus the twelve terms of (6.62) become

$$\begin{aligned}\langle|\mathcal{M}_{fi}|^2\rangle = 4\frac{Q_{\mathrm{f}}^2e^4}{q^4}\Big[&(p_1\cdot p_4)(p_2\cdot p_3) - (p_1\cdot p_2)(p_3\cdot p_4) + (p_1\cdot p_3)(p_2\cdot p_4)\\ &- (p_1\cdot p_2)(p_3\cdot p_4) + 4(p_1\cdot p_2)(p_3\cdot p_4) - (p_1\cdot p_2)(p_3\cdot p_4)\\ &+ (p_1\cdot p_3)(p_2\cdot p_4) - (p_1\cdot p_2)(p_3\cdot p_4) + (p_1\cdot p_4)(p_2\cdot p_3)\\ &- m_{\mathrm{f}}^2(p_1\cdot p_2) + 4m_{\mathrm{f}}^2(p_1\cdot p_2) - m_{\mathrm{f}}^2(p_1\cdot p_2)\Big],\end{aligned}$$

which simplifies to

$$\langle|\mathcal{M}_{fi}|^2\rangle = 4\frac{Q_{\mathrm{f}}^2e^4}{q^4}\Big[2(p_1\cdot p_3)(p_2\cdot p_4) + 2(p_1\cdot p_4)(p_2\cdot p_3) + 2m_{\mathrm{f}}^2(p_1\cdot p_2)\Big].$$

In the limit where the electron mass is neglected, the four-momentum squared of the virtual photon is

$$q^2 = (p_1 + p_2)^2 = p_1^2 + p_2^2 + 2(p_1\cdot p_2) \approx 2(p_1\cdot p_2),$$

and therefore

$$\langle|\mathcal{M}_{fi}|^2\rangle = 2\frac{Q_{\mathrm{f}}^2e^4}{(p_1\cdot p_2)^2}\Big[(p_1\cdot p_3)(p_2\cdot p_4) + (p_1\cdot p_4)(p_2\cdot p_3) + m_{\mathrm{f}}^2(p_1\cdot p_2)\Big]. \quad (6.63)$$

If the final-state fermion mass is also neglected, (6.63) reduces to the expression for the spin-averaged matrix element squared of (6.25), which was obtained from the helicity amplitudes.

In the above calculation, neither the explicit form of the spinors nor the specific representation of the $\gamma$-matrices is used. The spin-averaged matrix element squared is determined from the completeness relations for the spinors and the commutation and Hermiticity properties of the $\gamma$-matrices alone.

## $e^+e^- \to f\bar{f}$ annihilation close to threshold

The spin-averaged matrix element squared of (6.63) can be used to calculate the cross section for $e^+e^- \to f\bar{f}$ close to threshold. Working in the centre-of-mass frame and writing the momenta of the final-state particles as $p = \beta E$, where $\beta = v/c$, the four-momenta of the particles involved can be written

$$\begin{aligned}p_1 &= (E, 0, 0, +E),\\ p_2 &= (E, 0, 0, -E),\\ p_3 &= (E, +\beta E\sin\theta, 0, +\beta E\cos\theta),\\ p_4 &= (E, -\beta E\sin\theta, 0, -\beta E\cos\theta),\end{aligned}$$

and the relevant four-vector scalar products are

$$\begin{aligned} p_1 \cdot p_3 &= p_2 \cdot p_4 = E^2(1 - \beta\cos\theta), \\ p_1 \cdot p_4 &= p_2 \cdot p_3 = E^2(1 + \beta\cos\theta), \\ p_1 \cdot p_2 &= 2E^2. \end{aligned}$$

Substituting these expressions into (6.63) gives

$$\begin{aligned} \langle|\mathcal{M}_{fi}|^2\rangle &= 2\frac{Q_\mathrm{f}^2 e^4}{4E^4}\left[E^4(1-\beta\cos\theta)^2 + E^4(1+\beta\cos\theta)^2 + 2E^2 m_\mathrm{f}^2\right] \\ &= Q_\mathrm{f}^2 e^4\left(1 + \beta^2\cos^2\theta + \frac{E^2 - \mathrm{p}^2}{E^2}\right) \\ &= Q_\mathrm{f}^2 e^4\left(2 + \beta^2\cos^2\theta - \beta^2\right). \end{aligned} \tag{6.64}$$

The differential cross section is then obtained by substituting the spin-averaged matrix element squared of (6.64) into the cross section formula of (3.50) to give

$$\begin{aligned} \frac{\mathrm{d}\sigma}{\mathrm{d}\Omega} &= \frac{1}{64\pi^2 s}\frac{\mathrm{p}}{E}\langle|M_{fi}|^2\rangle \\ &= \frac{1}{4s}\beta Q_\mathrm{f}^2\alpha^2\left(2 + \beta^2\cos^2\theta - \beta^2\right), \end{aligned}$$

where $e^2 = 4\pi\alpha$. The total cross section is obtained by integrating over $\mathrm{d}\Omega$, giving

$$\sigma(\mathrm{e}^+\mathrm{e}^- \to \mathrm{f}\bar{\mathrm{f}}) = \frac{4\pi\alpha^2 Q_\mathrm{f}^2}{3s}\beta\left(\frac{3-\beta^2}{2}\right) \quad \text{with} \quad \beta^2 = \left(1 - \frac{4m_\mathrm{f}^2}{s}\right). \tag{6.65}$$

Close to threshold, the cross section is approximately proportional to the velocity of the final state particles. Figure 6.12 shows the measurements of the total $\mathrm{e}^+\mathrm{e}^- \to \tau^+\tau^-$ cross section at centre-of-mass energies just above threshold. The data are in good agreement with the prediction of (6.65). In the relativistic limit where $\beta \to 1$, the total cross section of (6.65) reduces to the expression of (6.24).

### 6.5.5 Electron–quark scattering

The main topic of the next two chapters is electron–proton scattering. In the case of *inelastic* scattering where the proton breaks up, the underlying QED process is $t$-channel scattering of electrons from the quarks inside the proton. In the limit

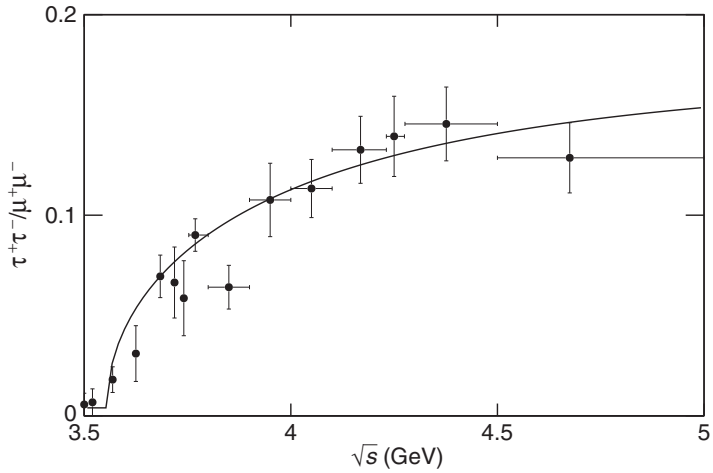


**Fig. 6.12** The measured ratio of number of identified $e^+e^- \to \tau^+\tau^-$ events to the number of $e^+e^- \to \mu^+\mu^-$ at centre-of-mass energies close to the $e^+e^- \to \tau^+\tau^-$ threshold. The curve shows the $\beta(3-\beta^2)$ behaviour of (6.65). The normalisation depends on the efficiency for identifying $\tau^+\tau^-$ events and a small background component is included. Adapted from Bacino *et al.* (1978).

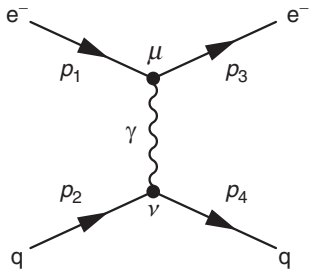


**Fig. 6.13** The lowest-order Feynman diagram for QED $t$-channel electron–quark scattering process.

where the masses of the electron and the quark can be neglected, it is relatively straightforward to obtain the expressions for the four non-zero matrix elements using the helicity amplitude approach (see Problem 6.7). However, if the particle masses cannot be neglected, which is the case for low-energy electron–proton scattering, the spin-averaged matrix element is most easily calculated using the trace formalism introduced above.

The QED matrix element for the Feynman diagram of Figure 6.13 is

$$\mathcal{M}_{fi} = \frac{Q_q e^2}{q^2} \left[\overline{u}(p_3)\gamma^\mu u(p_1)\right] g_{\mu\nu} \left[\overline{u}(p_4)\gamma^\nu u(p_2)\right] .$$

Noting the order in which the spinors appear in the matrix element (working backwards along the arrows on the fermion lines), the spin-summed matrix element squared is given by

$$\sum_{\text{spins}} |\mathcal{M}_{fi}|^2 = \frac{Q_\text{q}^2 e^4}{q^4} \text{Tr}\left([\not{p}_3 + m_\text{e}]\gamma^\mu[\not{p}_1 + m_\text{e}]\gamma^\nu\right) \text{Tr}\left([\not{p}_4 + m_\text{q}]\gamma_\mu[\not{p}_2 + m_\text{q}]\gamma_\nu\right) . \tag{6.66}$$

Apart from the signs of the mass terms, which are all positive since only particles are involved, the expressions in the traces of (6.66) have the same form as those of (6.60) and can therefore be evaluated using the result of (6.61) with the signs of the $m^2$ terms reversed, giving

$$\sum_{\text{spins}} |\mathcal{M}_{fi}|^2 = \frac{16\, Q_\text{q}^2 e^4}{q^4} \left(p_3^\mu p_1^\nu - g^{\mu\nu}(p_1\cdot p_3) + p_1^\mu p_3^\nu + m_\text{e}^2 g^{\mu\nu}\right) \times \left(p_{4\mu} p_{2\nu} - g_{\mu\nu}(p_2\cdot p_4) + p_{2\mu} p_{4\nu} + m_\text{q}^2 g_{\mu\nu}\right).$$

From this expression, it follows that

$$\begin{aligned} \langle|\mathcal{M}_{fi}|^2\rangle &= \frac{1}{4}\sum_{\text{spins}} |\mathcal{M}_{fi}|^2 \\ &= \frac{8Q_\text{q}^2 e^4}{(p_1 - p_3)^4} \times \Big[(p_1\cdot p_2)(p_3\cdot p_4) + (p_1\cdot p_4)(p_2\cdot p_3) \\ &\qquad - m_\text{e}^2(p_2\cdot p_4) - m_\text{q}^2(p_1\cdot p_3) + 2m_\text{e}^2 m_\text{q}^2\Big]. \end{aligned} \tag{6.67}$$

In the limit where the masses can be neglected, (6.67) reduces to

$$\langle|\mathcal{M}_{fi}|^2\rangle = 2Q_\text{q}^2 e^4 \left(\frac{s^2 + u^2}{t^2}\right). \tag{6.68}$$

Apart from the factor $Q_\text{q}^2$ from the quark charge, this spin-averaged matrix element squared for the $t$-channel scattering process of $\text{eq} \to \text{eq}$ is identical to the corresponding expression for $\text{e}^+\text{e}^- \to \mu^+\mu^-$ annihilation of (6.26) with $s$ and $t$ interchanged. The similarity between these two expressions is to be expected from the closeness of the forms of the fermion currents for the two processes. This property, known as crossing symmetry, can be utilised to obtain directly the expression for the spin-averaged matrix element squared for a $t$-channel process from that of the corresponding $s$-channel process.

### 6.5.6 Crossing symmetry

The calculations of the spin-averaged squared matrix elements for the $s$-channel $\text{e}^+\text{e}^- \to \text{f}\bar{\text{f}}$ annihilation process and the $t$-channel $\text{e}^-\text{f} \to \text{e}^-\text{f}$ scattering processes, shown in Figure 6.14, proceed in similar way. In the annihilation process, the two currents are

$$j_\text{e}^\mu = \bar{v}(p_2)\gamma^\mu u(p_1) \quad \text{and} \quad j_\text{f}^\nu = \bar{u}(p_3)\gamma^\nu v(p_4), \tag{6.69}$$

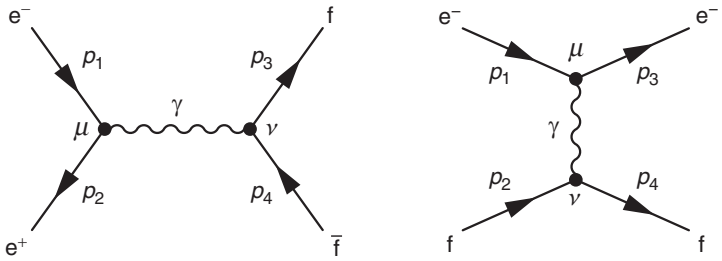


**Fig. 6.14** The Feynman diagrams for QED $s$-channel annihilation process $e^+e^- \to f\bar{f}$ and the QED $t$-channel scattering process $e^-f \to e^-f$.

and for the scattering process the corresponding two currents are

$$j_e^\mu = \bar{u}(p_3)\gamma^\mu u(p_1) \quad \text{and} \quad j_f^\nu = \bar{u}(p_4)\gamma^\nu u(p_2). \tag{6.70}$$

By making the replacement $u(p_1) \to u(p_1)$, $\bar{v}(p_2) \to \bar{u}(p_3)$, $\bar{u}(p_3) \to \bar{u}(p_4)$ and $v(p_4) \to u(p_2)$ the currents in the annihilation process (6.69) correspond to those for the scattering process (6.70). In the calculation of traces, this implies making the replacement, $p_1 \to p_1$, $p_2 \to p_3$, $p_3 \to p_4$ and $p_4 \to p_2$. This accounts for the order in which the spinors appear in the four-vector currents, but does not account for the replacement of an antiparticle spinor with a particle spinor. From the completeness relationships of (6.40) and (6.41), the spin sums lead to a term in the trace of $[\not{p} + m]$ for particles and $[\not{p} - m]$ for antiparticles. So when a particle is replaced by an antiparticle, the sign of the mass term in the trace is reversed. Alternatively, the effect of changing the *relative* sign between $\not{p}$ and $m$, can be achieved by changing the sign of the four-momentum when a particle in one diagram is replaced by an antiparticle in the other diagram. Hence, crossing symmetry implies that the matrix element for $e^-f \to e^-f$ can be obtained the matrix element for $e^+e^- \to f\bar{f}$ by making the substitutions,

$$p_1 \to p_1, \quad p_2 \to -p_3, \quad p_3 \to p_4 \quad \text{and} \quad p_4 \to -p_2.$$

The effect on the Mandelstam variables is $s^2 \to t^2$, $t^2 \to u^2$ and $u^2 \to s^2$, and with these replacements the matrix element for the $s$-channel annihilation process $e^+e^- \to f\bar{f}$ of (6.26) transforms to the matrix element for the $t$-channel scattering process $e^-f \to e^-f$ of (6.68)

$$\langle|\mathcal{M}_{fi}|^2\rangle_s = 2Q_f^2 e^4\left(\frac{t^2+u^2}{s^2}\right) \quad \longleftrightarrow \quad \langle|\mathcal{M}_{fi}|^2\rangle_t = 2Q_f^2 e^4\left(\frac{u^2+s^2}{t^2}\right).$$

## Summary

In this chapter, the $e^+e^- \to \mu^+\mu^-$ annihilation process has been used to introduce the techniques used to perform lowest-order QED calculations. A number of important concepts were introduced. The treatment of the different spin states of the initial- and final-state particles leads to the introduction of the spin-averaged matrix element squared given by

$$\langle |\mathcal{M}_{fi}|^2 \rangle = \frac{1}{4} \sum_{\text{spins}} |\mathcal{M}|^2,$$

where the sum extends over the sixteen orthogonal spins states. In the limit where the masses of the particles were neglected, only four of the possible helicity combinations give non-zero matrix elements. This property is due to the chiral nature of the QED interaction, where the left- and right-handed chiral states are eigenstates of the $\gamma^5$-matrix defined as

$$\gamma^5 \equiv i\gamma^0\gamma^1\gamma^2\gamma^3.$$

Because of the $\bar{\phi}\gamma^\mu\psi$ form of the QED interaction vertex, certain combinations of chiral currents are *always* zero, for example $\bar{u}_R\gamma^\mu u_L = 0$. In the limit $E \gg m$, the helicity eigenstates correspond to the chiral eigenstates and twelve of the sixteen possible helicity combinations in the process $e^+e^- \to \mu^+\mu^-$ do not contribute to the cross section and helicity is *effectively* conserved in the interaction. The resulting spin-averaged matrix element squared for $e^+e^- \to \mu^+\mu^-$ is

$$e^+e^- \to \mu^+\mu^- : \quad \langle |\mathcal{M}_{fi}|^2 \rangle = 2e^4 \left( \frac{t^2 + u^2}{s^2} \right). \tag{6.71}$$

In the starred section of this chapter, the method of using traces to perform spin sums was introduced and was then used to calculate the matrix elements for $e^+e^- \to f\bar{f}$ annihilation and $e^-q \to e^-q$ scattering. In the massless limit, the spin-averaged matrix element squared for electron–quark scattering was shown to be

$$e^-q \to e^-q : \quad \langle |\mathcal{M}_{fi}|^2 \rangle = 2Q_q^2 e^4 \left( \frac{s^2 + u^2}{t^2} \right). \tag{6.72}$$